ANALYSIS OF RE-ENTRY EVENT OF CZ-3B R/B OBSERVED BY ALL-SKY METEOR CAMERAS AMOS

J. Šilha[1,2], D. Bartková[1,2], P. Jevčák[1,2], D. Kyselica[1], V. Pazderová[1], P. Matlovič[1], J. Tóth[1], L. Kornoš[1], T. Hrobár[1], R. Ďurikovič[1], P. Poláček[3], S. Lemmens[4], and B. Jilete[4]

[1] *Faculty of Mathematics, Physics, and Informatics, Comenius University Bratislava, Mlynska dolina, 842 48 Bratislava, Slovakia, Email: daniela.bartkova@fmph.uniba.sk*

[2] *Astros Solutions s.r.o., Nad Lúčkami 3141/35, 84 105, Bratislava, Slovakia, Email: jiri.silha@astros.eu*

[3] *Armed Forces Academy of general Milan Rastislav Štefánik, Demänová 393, 031 01 Liptovský Mikuláš 1, Slovakia*

[4] *ESA/ESOC, Space Debris Office, Robert-Bosch-Strasse 5, DE-64293 Darmstadt, Germany*

ABSTRACT

A re-entry event was captured on October 24^{th} 22:01 HST (October 25^{th} 08:01:37 UTC) by the automated meteor cameras AMOS on the Haleakalā and Maunakea Observatories in Hawaii. The re-entering rocket body CZ-3B R/B (2008-055B), used to launch VENESAT-1 in 2008, and its fragments were visible as a rapidly moving group of meteor-like light sources leaving trails crossing the entire night sky. The event was recorded by two AMOS all-sky video systems and a high-resolution spectral camera, that captured the given event in more detail. In the presented work we will discuss the reduction of the obtained video recordings and the current status of the physical and dynamical properties of detected fragments.

Keywords: re-entry; meteor all-sky cameras, atmospheric trajectory, light curves.

1. INTRODUCTION

1.1. Re-entry events

Re-entries of satellites and upper stages, which are events accompanied by ablation and disintegration process, are becoming quite common phenomena. To the ground-based observer, they appear similar to meteors caused by meteoroids. It is expected these events will be more frequently detected by all-sky meteor systems which are redistributed around the world. Fig. 1 depicts the histogram for upcoming re-entry events, mass as a function of a number of objects per bin. Fig. 1 was generated by ESA using the LASCO (Lifetime Assessment of Catalogued Objects) tool [5] (to January 2023). LASCO predicts that more than 1370 cataloged objects will re-enter the atmosphere as controllable and uncontrollable in the next three years, which is around 9 potential artificial meteor-like phenomena per week. However, this number does not account for the upcoming missions to take place in the next three years. From those, almost 100 objects have a mass large than 1 metric ton, which is on average one large object to re-enter every 1.5 weeks.

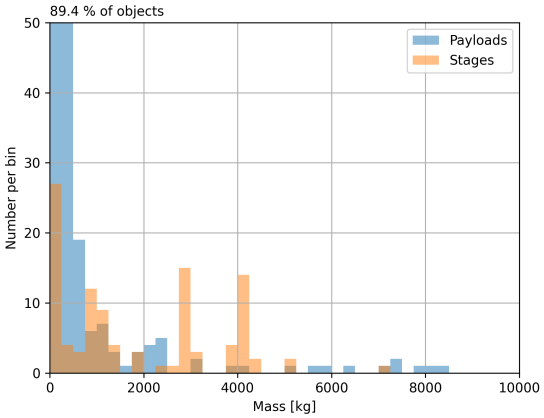

Figure 1. Number of objects expected to re-enter the atmosphere uncontrollably in time period January 2023 and January 2025. Data generated by ESA LASCO tool (to January 2023). Bin width = 250kg. [5]

One of the orbital elements which mostly influences the area, or geodetic latitude where the object is going to re-enter and its fragments potentially to fall, is orbital inclination. In Fig. 2 is shown mass vs. inclination for all LASCO objects. It is clear that the majority of the objects have retrograde orbits with inclinations between 95°- 105°.

A significant part (almost 60 %) of the objects to re-enter in the next three years and are heavier than 1 metric ton are rocket upper stages. One type of upper stage which is commonly observed during re-entries is the third stage of

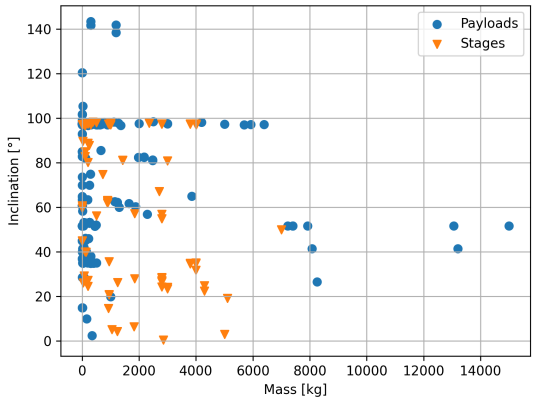

Figure 2. Mass vs. orbital inclination of the objects expected to re-enter the atmosphere uncontrollably in the time period between April 2022 and April 2025. Data generated by ESA LASCO tool (to January 2023). [5]

the Long-March 3 rocket, here referred to only as CZ-3B R/B, which has a cylindrical shape with a diameter of 3 m and height of 12.74 m and with an empty mass of around 2800 kg [1].

1.2. AMOS all-sky system

AMOS (All-Sky Meteor Orbit System) [14] is a passive optical sensor, developed and operated by the Faculty of Mathematics, Physics and Informatics of the Comenius University in Bratislava, Slovakia. It is an intensified video meteor detection system covering almost all-sky for continuous automatic monitoring of the meteor activity in the atmosphere.

The limiting magnitude for stars is about $+5\ ^{mag}$ for a single frame, the efficiency is lower for moving objects approx. $+4\ ^{mag}$, due to the trailing lost. The operation of cameras is automatic but can be remotely controlled through internet connection. The entire system is protected by outer and inner enclosures and is secured by environmental detectors for temperature, humidity, rain and illumination of the sky.

Currently, there are 21 operational AMOS cameras in total, 10 in Slovakia and 11 abroad (Fig. **??**), specifically on Canary Islands with the cooperation of IAC, Chile (SpaceObs, Paniri Caur Observatories), on Hawaii (Haleakala and Maunakea Observatories, IfA Univ. of Hawaii, SMA CfA), in Australia (Mundrabilla, Forrest, Kybo, Curtin University Perth) and in South Africa (Sutherland Observatory, Cederberg Amateur Observatory). In addition to the standard AMOS systems (AMOS-Cam), used for meteor trajectory and orbit determination, the network currently includes 5 spectral systems (AMOS-Spec). Each location operates pair of AMOS cameras (except for 3 AMOS in Australia) and AMOS-Spec for spectroscopy [10], enabling spectral and compositional characterization of the incoming objects. AMOS-Cam could be also used for meteorological, geophysical, aviation or satellite observations. The direct distance between individual stations within one location ranges from 80 to 150 km.

Figure 3. Geographical positions of AMOS in Slovakia and in the AMOS Global Meteor Network (red crosses - installed, blue crosses – planned).

1.3. Re-entry event of CZ-3B R/B

On October 25^{th} 2020 at 08:01:37 UTC, two of the AMOS all-sky cameras situated on the Haleakalā (AMOS-HK) and Maunakea (AMOS-MK) Observatories in Hawaii captured the re-entry of a rocket body CZ-3B R/B (2008-055B). Both AMOS-HK and AMOS-MK recorded a significant portion of the CZ-3B R/B re-entry event - more than 50 seconds long video recordings showing a gradually expanding cloud of fragments. The composite images of the video recordings captured from AMOS-HK and AMOS-MK are shown in Fig. 4 and Fig. 5, respectively.

Figure 4. Composite image of CZ-3B re-entry video recording captured by AMOS-HK on October 25^{th} 2020 at 08:01:39 UTC. Duration of recording is 51.65 s and it contained 1033 frames. The arrow on the image marks a sudden increase in brightness around 1 minute before the video recording.

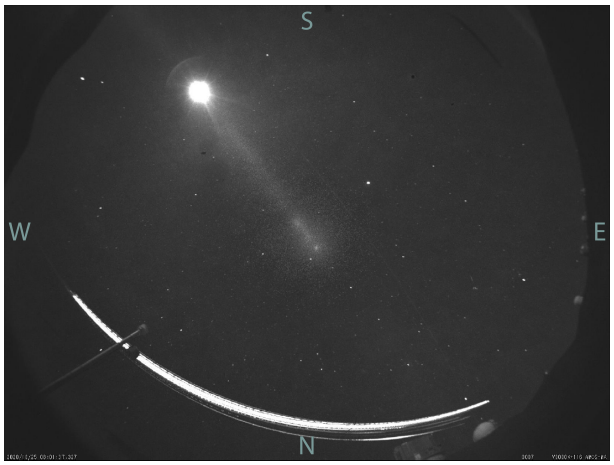

Figure 5. Composite image of CZ-3B re-entry video recording captured by AMOS-MK on October 25^{th} 2020 at 08:01:37 UTC. Duration of recording is 56.15 s and it contained 1123 frames.

2. IMAGE REDUCTION

2.1. Segmentation

The measurement of positions and intensity of individual fragments was done using a custom program AMOS-Capture S/W [14], originally developed for the detection and tracking of meteors captured by the AMOS network. The software detects moving objects and background stars, whose coordinates and intensities are needed later for astrometric and photometric reduction. Once a moving object is detected, the software tracks its position frame-by-frame. The position of a moving object and/or a static star is estimated by the method of Gaussian fitting, acquiring its rectangular (pixel) coordinates, corresponding to the center of the fitted Gaussian.

2.2. Astrometric and photometric reduction

MeteorTrajectory S/W [7] is a custom software for astrometric and photometric reduction, and meteor trajectory and orbit calculation, used for the analysis of meteors observed by AMOS. The plate solving is based on the Borovička all-sky astrometric reduction [3]. The photometric reduction is performed using reference stars cross correlation between the catalogue and instrumental brightness. There is also applied a correction for the atmospheric extinction and vigneting of the fish-eye. Trajectory calculation is based on the method of intersecting planes [6], which assumes linear trajectory. Previous analysis of CZ-3B re-entry event [11] resulted in confirmation that this assumption is inappropriate when dealing with re-entering space debris since these objects are slower and more affected by Earth's gravity, which curves their trajectories through the atmosphere. Thus, within this work, we present a new approach (Section 2.5), using this S/W only for the astrometric reduction. Additionally, MeteorTrajectory S/W is commonly used for the object association between two recordings. However, routine processing, as experimental algorithms [11] showed, that manually done association with human-in-loop for a large number of fragments is the preferable option to perform this step (Section 2.4).

2.3. Photometric light curves

Measured light curves of individual fragments contain additional information. They can be used for the estimation of a fragment's size and mass and their change with time or altitude (after trajectory estimation). Conversion from instrumental intensity to magnitudes is done during astrometric reduction using MeteorTrajectory S/W. We were able to extract 34 light curves in total, 17 for each station. The light curve of the front fragment acquired from both stations is shown in Fig. 6.

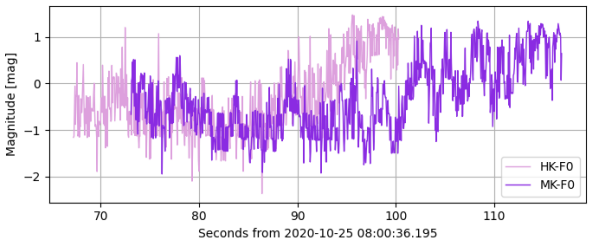

Figure 6. Light curve of the front fragment, designated HK-F0 and MK-F0.

2.4. Object association between recordings

Since at least two-station position measurements are needed for the trajectory estimation to exploit the triangulation, each fragment with measured positions has to be associated between two recordings obtained from two different locations. It turned out that the best tool for the association so far is the human eye, trained to recognize the spatial character of a moving object from changing perspective. This is known as the *effect of parallax*. By replaying the video recordings at a higher playback speed, the change of perspective is clearly visible as the cluster of fragments crosses the sky from west to east. For AMOS-HK, the cluster moved almost through the zenith, offering a view of the cluster from below it, expecting that if one fragment is apparently moving faster compared to the whole cluster, it is located closer to the observer, hence at the bottom of the cluster. This behavior is depicted in Fig. 10, where the circles mark fragments with the highest apparent angular velocities observed by AMOS-HK. Additionally, since the orientation of the station is known, we could also determine which fragments are at the north and the south side of the cluster. For AMOS-MK, located south of AMOS-HK, the cluster moved closer to the horizon in the northern part

of the celestial sphere, offering a view of the cluster from its south side. Thus, by analogy, it is possible to identify fragments on the south side and associate them with fragments from the AMOS-HK recording. With this method, it was possible to associate 6 pairs of fragments. The association of 5 fragments forming the front sub-cluster and one bright fragment at the tail of the cluster was straightforward.

Another 4 fragments were associated using photometry described in Section 2.3. Comparing light curves from the two stations, one can look for similar photometric behavior, mostly the period of regular changes. Some fragments show regular flickering, which is seen from both stations. This behavior is also seen in the light curve, thus it is possible to plot two curves together and see whether the periods match. An example is shown in Fig. 7. The association can be verified based on the absolute magnitude obtained after trajectory estimation since the distance from the station is needed to calculate the absolute magnitude of a fragment.

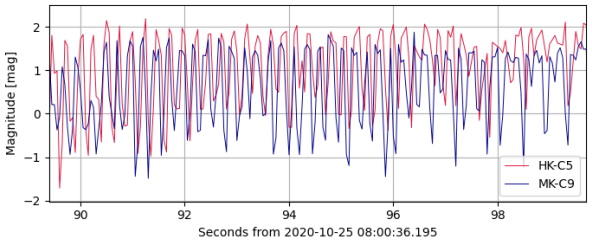

Figure 7. Section of the light curve of a single associated fragment with designations HK-C5 (seen from AMOS-HK) and MK-C9 (seen from AMOS-MK). The periods of flickering match up, indicating that it is the same object.

Light curves shown in Fig. 7 have been processed by using FMPI's internal tool to extract the apparent periods [12] to further confirm the similarities between both data sets. We were able for both cases to construct the phase diagram, which is the light curve folded to the found apparent rotation period. Diagrams are shown in Fig. 8 and Fig. 9. For the fragment AMOS-HK-C5 we extracted apparent period to be 0.505±0.01 s and apparent amplitude of the signal to be 3.7±0.01 mag. For the fragment AMOS-MK-C9 we extracted apparent period to be 0.503±0.01 s and apparent amplitude of the signal to be 3.5±0.01 mag. Both signals show very similar parameters and therefore it could be concluded that they belong to the same object.

2.5. Trajectory estimation by lines-of-sight method

An alternative to the intersecting planes is the least-square method described in [2]. It finds the optimal trajectory by minimizing the distances of a straight line to the lines of sight, emanating from each station. This approach can be extended to assume a curved path. The proposed approach is illustrated in Fig. 11. With a cus-

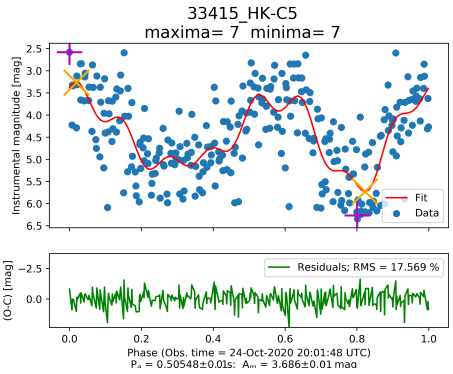

Figure 8. Reconstructed period phase diagram using estimated apparent period for the fragment AMOS-HK-C5.

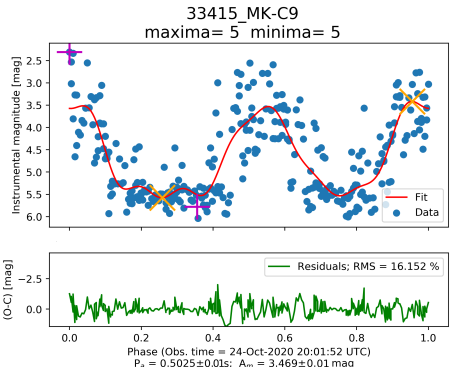

Figure 9. Reconstructed period phase diagram using estimated apparent period for the fragment AMOS-MK-C9.

tom code written in Python, we calculated the geocentric 3D coordinates of the intersections (or the closest points) between two lines of sight, each measured for a single fragment (azimuth and elevation above the horizon estimated during the plate solving discussed in Section 2.2) from a single station. The distance between the two points is minimal only for one pair of lines of sight, which are geometrically closest in 3D space. The result is a sequence of points for each station, approximately defining the observed trajectory. The coordinates are in an Earth-centered non-rotating frame but can be transformed into other frames (geodetic coordinates are preferred). We accounted for the changing coordinates of the stations in this frame, in which they are not stationary.

Fig. 12 shows the resulting altitudes of 4 example fragments and their change with time. The curves have the expected shape (curving downwards), commonly seen in re-entry modeling results, confirming that the applied method, though yet not comprehensive, gives more satisfactory results than the intersecting planes method. The altitudes attest to our assumption about the spatial distribution of the given fragments - the lowest fragment, designated HK-B0 and MK-B0 (orange line), is the one considered to be the first one from the bottom of the cluster, followed by HK-B1/MK-C8 (yellow line), the second from the bottom. Fragment HK-S0/MK-C7 (red line) is

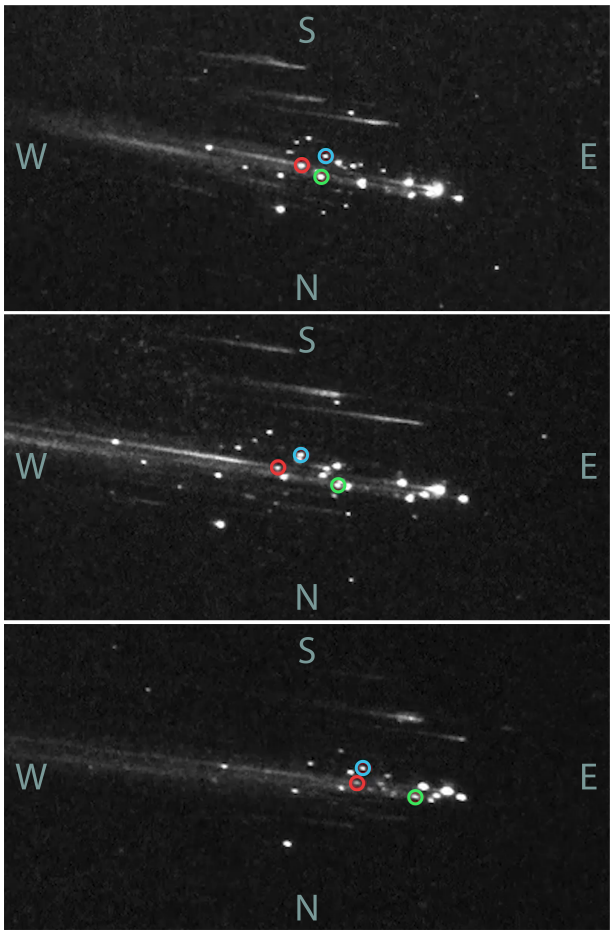

Figure 10. Changing perspective of the CZ-3B re-entry cluster captured by the all-sky AMOS camera at Haleakalā in three different chronologically ordered moments in time. The colored circles mark three fragments whose apparent position within the cluster changes. While the red and blue fragments stay close to each other, changing their relative position a little, the green one crosses from the center of the cluster to the front. This is caused by the change of perspective, not because it has a higher velocity.

located at the south side of the cluster, separated from the central region. The steepness of the altitude decrease with time is related to the physical properties of the fragments.

3. INITIAL ANALYSIS WITH ESA DRAMA TOOL

Debris Risk Assessment and Mitigation Analysis (DRAMA) tool, developed by ESA [4], consists of several modules, each dealing with different problems during the life of a spacecraft in its orbit, e.g. risk events (possible collisions), meteoroids impacts, orbital lifetime, disposal options, re-entry survival, impact footprint, and casualty probability. The *re-entry Survival And Risk Analysis* (SARA) tool within DRAMA models

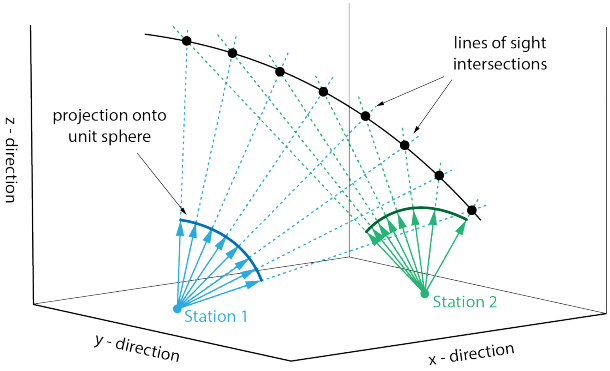

Figure 11. Illustration of intersecting lines of sight. In an ideal case with highly precise time-synchronized observations of a meteor/re-entry fragment fall, the lines of sight emanating from each station would intersect in a single point in 3D space, lying on the real trajectory of the object. In reality, the intersection does not exist.

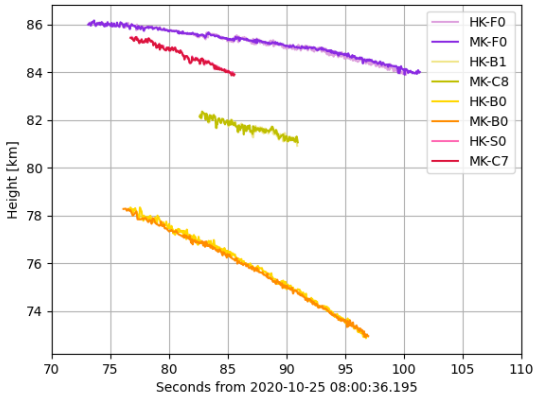

Figure 12. Altitude vs. time for 4 example fragments. Time 2020-10-25 08:00:36.195 is the time of sudden flash recorded by AMOS-HK (see Fig. 4).

the re-entry of the spacecraft based on initial conditions set by the user. The main body can have an arbitrary number of components, defined by simple shapes, which are analyzed independently after the breakup of the main body. SARA uses aerodynamic, aerothermodynamic, and ablation models to simulate the object's and its components' trajectory and dynamical and physical parameters during the re-entry.

3.1. Initial simulation

We did a preparatory simulation of the 3^{rd} stage of CZ-3B re-entry with the DRAMA/SARA tool for comparison with the results from the previous section. The model rocket body had physical properties as stated in Section 1.1. Due to the lack of information about its internal components, we assumed a single child object - a hollow sphere with 50 cm diameter and a mass of 7 kg, ac-

cording to debris retrieval of another CZ-3B fall in 2018 (Paraguay) [15]. The child was set to be released at 95 km with Δv=0.1 km/s. Orbital parameters of the rocket body were extracted from the last registered TLE, obtained from [13]. Results of the simulation are shown in Fig. 13.

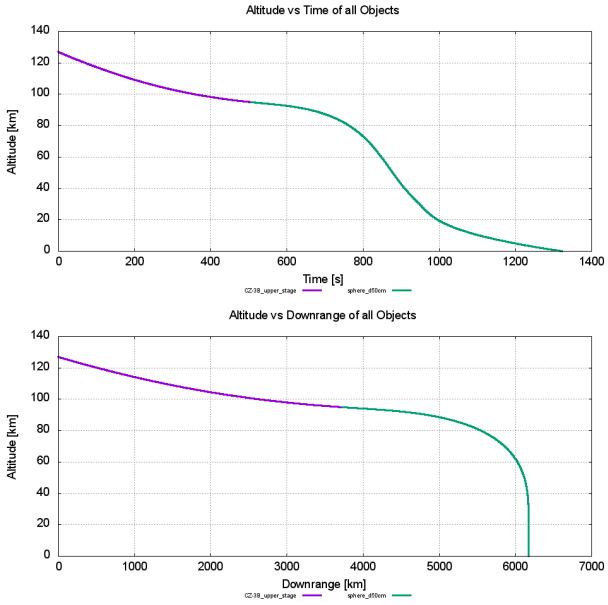

Figure 13. Altitude vs. time (top) and downrange (bottom) for the 3^{rd} stage of CZ-3B (purple line) and the 50 cm sphere set to release from the main body at 95 km (green line).

3.2. Breakup altitude estimation

We used the results to estimate the altitude at which the recorded sudden flash might have happened. By taking the computed trajectory of the front fragment (HK-F0) and shifting the results from DRAMA in time by a δt, for which the residuals between the fragment's altitude and the sphere's altitude were minimal, we obtained a fit to the fragment's altitude as a function of time. Note that the time in results from DRAMA is counted from the epoch of used TLE, which is 2020-10-25 05:11:43.589 UTC - approximately 3 hours sooner than the observations. The time of the fragment's first measurement is known, thus we can determine the altitude the fragment had at the time of the sudden flash from the fit (see Fig. 14). This approach is only the first attempt to determine the altitude of the breakup. The fit to a fragment's trajectory has to be more sophisticated in order to get satisfactory results when extrapolating it backward in time, or it should be done utilizing dynamical models rather than considering only the geometry of the observed path. An accurate fit is also needed for velocity and deceleration calculated from the measured trajectory.

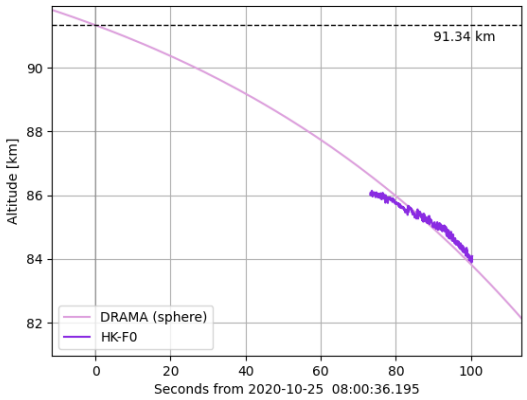

Figure 14. Comparison of front fragment attitude vs. time and the altitude calculated by DRAMA assuming 50 cm spherical fragment.

4. CONCLUSIONS AND NEXT STEPS

The presented work focused on the data reduction of video recordings acquired by the AMOS all-sky cameras of the CZ-3B R/B which re-entered over Hawaii in October 2020. The primary objective is to extract measurements of fragments visible in each recording, then associate fragments between recordings and construct their light curves and atmospheric trajectories. We identified inadequate steps in the existing procedure used primarily for meteor observations. We were able to construct trajectories and light curves for 16 fragments and presented one example in this work. In future work, we will focus on the dynamical modeling of the fragments, including also atmospheric and aerodynamic models. We will Investigate ablation coefficients and masses of the observed fragments, as well as the model presumed fragmentation event which might have occurred, according to the observations around 60 s prior to the video recordings.

ACKNOWLEDGMENTS

This work has been supported by ESA Contract no. 4000136672/21/NL/SC - Validation of re-entry models by using real optical measurements obtained by AMOS global network.

REFERENCES

1. Astronautix.com (2023) "Chang Zheng 3B". *http://www.astronautix.com/c/changzheng3b.html*.
2. Borovička J. (1990) "The Comparison of Two Methods of Determining Meteor Trajectories from Photographs". *Bulletin of the Astronomical Institute of Czechoslovakia*, **41**, 391-396.

3. Borovička J., Spurný P., and Keclíková J. (1995) "A new positional astrometric method for all-sky cameras". *Astronomy and Astrophysics Supplement*, **112**, 173-178.

4. Braun V., Funke Q., Lemmens S. and Sanvido S. (2020) "DRAMA 3.0 - Upgrade of ESA's debris risk assessment and mitigation analysis tool suite". *Journal of Space Safety Engineering*, **7**, 206-212.

5. Bunte, K., Sdunnus, H. Mandeville, J. Klinkrad, H. (2001) "Ballistic parameter and lifetime assessment for catalogued objects". In *Proceedings of 3rd European Conference on Space Debris*,**473**, 781-786.

6. Ceplecha Z. (1987) "Geometric, Dynamic, Orbital and Photometric Data on Meteoroids From Photographic Fireball Networks". *Bulletin of the Astronomical Institute of Czechoslovakia*, **38**, 222-234.

7. Ďuriš F., Kornoš L., and Tóth J. (2018) "MT: Software for calculating Meteor Trajectories and orbits from multiple-stations observations". In *Proceedings of the International Meteor Conference, Modra-Piesok, Slovakia*, 127-128.

8. Kornoš L., Ďuriš F., and Tóth J. (2015) "Astrometric precision and orbit determination by AMOS". In *Proceedings of the International Meteor Conference, Mistelbach, Austria*, 101-104.

9. Kornoš L., Ďuriš F., and Tóth J. (2018) "AMOS orbit software and EDMOND database". In *Proceedings of the International Meteor Conference, Petnica, Serbia*, 46-49.

10. Matlovič P., Tóth J., Kornoš L., Loehle S. (2020) "On the sodium enhancement in spectra of slow meteors and the origin of Na-rich meteoroids". In *Icarus*, Volume 347, 2020, 113817, ISSN 0019-1035, https://doi.org/10.1016/j.icarus.2020.113817.

11. Pazderová V., Šilha J., Matlovič P., Tóth J., Kornoš L., and Zigo P. (2021) "Re-entry event of CZ-3B R/B observed by all-sky meteor cameras AMOS". In *Advance Maui Optical and Space Surveillance Technologies Conference (AMOS)*.

12. Šilha, J., Krajčovic, S., Zigo, M., et al. (2020). Space debris observations with the Slovak AGO70 telescope: Astrometry and light curves. Advances in Space Research. doi: https://doi.org/10.1016/j.asr.2020.01.038.

13. *https://www.space-track.org/*

14. Tóth J., Kornoš L., Zigo P., Gajdoš Š., Kalmančok D., Világi J., Šimon J., Vereš P., Šilha J., Buček M., Galád A., Rusňák P., Hrábek P., Ďuriš F., and Rudawska R. (2015). "All-sky Meteor Orbit System AMOS and preliminary analysis of three unusual meteor showers". *Planetary and Space Science*, **118**, 102-106.

15. Watchers.news (2018) "CZ-3B rocket body re-entry recorded over Paraquay". *https://watchers.news/2018/03/12/cz-3b-rocket-body-re-entry-recorded-over-paraguay/*